https://doi.org/10.46813/2025-159-033

FEATURES OF MICROPOROSITY FORMATION WHEN IRRADIATING ALUMINUM ALLOYS BY HIGH-CURRENT PULSED ELECTRON BEAMS

V.V. Bryukhovetsky[1], D.E. Myla[1], V.V. Shatov[1], O.L. Rak[2], V.A. Bychko[3]
[1]Institute of Electrophysics and Radiation Technologies NAS of Ukraine, Kharkiv, Ukraine;
[2]NSC "Kharkiv Institute of Physics and Technology", Kharkiv, Ukraine;
[3]Chernihiv Polytechnic National University, Chernihiv, Ukraine
E-mail: ntcefo@yahoo.com

Different types of surface microporosity arising from irradiation of metals and alloys by high-current pulsed electron beams (HCPEB) were characterized in this study. Three types of such porosity were identified, namely: vacancy, shrinkage, and deformation porosity. The study also features the kinds of common types of such microporosity. The mechanisms of formation of each of the listed types of microporosity were analyzed. The significance of these observations for a deeper understanding of the structural-phase transformations occurring during irradiation of metals and alloys with pulsed electron beams is discussed.

PACS: 29.25.Bx, 61.80.Fe, 62.20.−x

INTRODUCTION

Recently, various technologies for creating hardening coatings using concentrated energy sources have attracted increasing interest in surface modification of metallic materials [1]. A high-current pulsed electron beam (HCPEB) is especially crucial among these methods [2–7]. This is due to the fact that the energy concentration in the pulse is very high and can vary over a rather large range. Consequently, any kind of heat effects on the near-surface layers of materials can be achieved, namely: heating, melting, and even high-speed vaporization. The extremely rapid heating and cooling process caused by the interaction of HCPEB with the material surface induces several physical and chemical phenomena that include melting, rapid solidification, vaporization, thermal stress generation, shock wave, and accelerated diffusion. All this leads to non-equilibrium solidification on the surface of the molten material, resulting in a specific surface modification effect that is unattainable with traditional surface treatment methods. The combination of the aforementioned factors can contribute to structural-phase transformations, melt any refractory components and compounds with their subsequent crystallization in the form of high-strength, wear-resistant, and corrosion-resistant phases, as well as obtain coatings of virtually any composition and purpose. Unfortunately, various defective structures are often formed on the irradiated surface when HCPEB irradiates metals and alloys, the main ones of which – craters and cracks – deteriorate the mechanical reliability of structural materials and limit the application of this method [3, 6, 8]. In addition, another phenomenon of such treatment, the formation of microporosity, has been detected and discussed in several studies [9–11]. The mechanisms of formation of such porosity are still not completely clear and are currently debatable. Therefore, the characteristics and types of surface microporosity in some metals and alloys irradiated by HCPEB are given and the possible mechanisms of formation of different types of such microporosity are discussed in this study, based on our own research and with the involvement of literature data.

1. EXPERIMENTAL

Aluminum-based alloys 1933, AA6111, and AA2024 were selected as the target material for the study. Plates with dimensions of 10 cm (width)×10 cm (length)×2.5 mm (thickness) were made for conducting experimental studies. One side surface of all plates was polished to a mirror shine. The polished plate surfaces were irradiated with a single HCPEB impulse at room temperature. Irradiation of the plates was performed by a HCPEB at the TEMP-A accelerator in the NSC KIPT of the NAS of Ukraine [3, 5, 7]. The energy flux density at the target W is approximately 10^9 W/cm^2 (beam energy $E \sim 0.35$ MeV, current $I \sim 2000$ A, pulse duration $\tau_i \sim 5 \cdot 10^{-6}$ s, beam diameter $D \sim 5$ cm). Irradiation was done by the single impulse in a vacuum at $1.3 \cdot 10^{-3}$ Pa. Microstructural studies were performed using optical microscopy (*Olympus* GX51) and scanning electron microscopy (JEOL ISM 820).

2. RESULTS AND DISCUSSION

The creation of certain structural and phase transformations caused by special types of their treatment is the basis of any modification of material properties. The essence of the main processes of stimulating changes in the structure of materials irradiated by HCPEB consists in high rates of heating of surface layers and their subsequent ultrafast cooling. In this case, in contrast to other processes based on temperature effects, the peculiarity of HCPEB irradiation is the property of relativistic electrons to penetrate deep into the target and create unevenly distributed heating. A detailed description of all structural components of the newly formed layer is crucial for a deep understanding of the physical processes leading to certain structural and phase states. Surface microporosity is one of the features of the surface relief formed after HCPEB irradiation [9–11]. Surface microporosity can have different sizes and shapes. However, very little attention has been paid to the study of this phenomenon. Therefore, there are several phenomenological approaches to explain the formation of surface microporosity during HCPEB irradiation. Previously, no study has analyzed and characterized the different types of surface microporosity. Only partial explanations of one or another of the reasons for the formation of such porosity have been given. The research carried out in this study, as well as a detailed analysis of the studies of many other authors allows us to distinguish three following types of such microporosity.

2.1. VACANCY POROSITY

Fig. 1 shows the types of surface morphology of HCPEB-irradiated AA6111 and 1933 aluminum alloys. The specimens in this figure are unpolished and retain a regular surface relief, which records the crystallization history of their surface after the action of a single HCPEB impulse. The main parameters of the surface morphology of these alloys were described earlier in studies [12–14]. Further studies of the HCPEB-modified surface of these alloys showed that the action of HCPEB is accompanied by the formation of a developed surface relief and the appearance of surface microporosity on it. Colonies of surface micropores are unevenly distributed. There are areas where such pores are quite numerous. However, there are areas on the irradiated surface where such micropores are completely absent. It was established that the micropores have a rounded shape with good dispersion and uniform size distribution. Most of the surface micropores are isolated from each other, and the micropore sizes are approximately 0.5…1.5 μm (see Fig. 1).

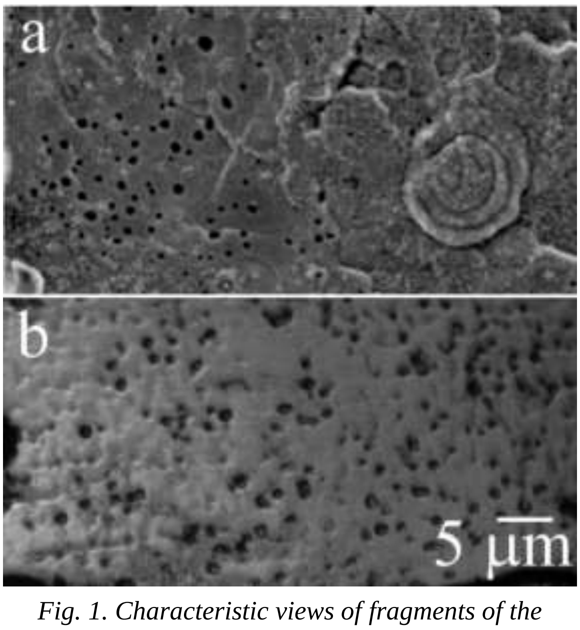

Fig. 1. Characteristic views of fragments of the irradiated surface of AA6111 alloy (a) and 1933 alloy (b)

It should be noted that the depth of surface micropores is variable and can reach 10 μm, while the thickness of the remelted layer is almost an order of magnitude greater. Most pores are oriented perpendicular to the surface, but there are also pores located at various angles relative to the surface.

This type of surface morphology is not entirely characteristic of HCPEB-irradiated materials. However, surface porosity was still observed in several studies [9–11, 15–18]. In the study [15], such porosity was observed on the irradiated surface of AISI 304 austenitic steel. It is noted [15] that there are areas with surface pore diameters of 1…2 μm and areas with pore diameters of 100…300 nm on the irradiated surface. At that, craters on the irradiated surface are practically absent. The same micropores smaller than 1 μm were observed in the study [16] when pure zirconia was irradiated. The authors also point to the fact that crater formation practically does not occur. However, it is noted [16] that fewer micropores are formed with more impulses. According to the authors [16] this is due to the fact that at a smaller number of impulses, there is a faster cooling of the molten surface and the spreading melt does not have time to fill the micropores. The formation of microporous elements on the irradiated surface of nickel [9], polycrystalline copper [10], and pure aluminum [11] was also observed.

As for the mechanisms of formation of such microporosity, the study [17] shows that at high quenching rates ($5 \cdot 10^9$ K/s) a large density of nonequilibrium vacancies migrated to the surface, where the near-surface structure of pure iron irradiated by HCPEB was studied. The concentration of formed nonequilibrium vacancies reached the value of 10^3 [17]. Initially, the maximum vacancy density was formed at a depth that corresponds to the maximum absorbed beam energy. It should be noted that in contrast to many processes based on temperature effects, the property of relativistic electrons to penetrate deep into the target and create a non-uniformly distributed heating with a maximum located approximately 1/3 of the depth of electron penetration is the determining factor in the irradiation by HCPEB [6]. While heat redistribution under the influence of temperature gradients takes place, the layer of material lying closer to the surface heats up faster, as the temperature of surface layers grows at a higher rate than the rate of its decrease in the inner part of the specimen body. As a result, most of the nonequilibrium vacancies migrate exactly to the surface. Dislocations and grain boundaries are the main pathways for vacancy migration. Apparently, this leads to the accumulation of vacancies near one-dimensional and two-dimensional defects in the surface layers of the specimen. Therefore, the local density of the material appears to decrease near such defects. On this basis, it was concluded in the study [17] that these areas with low local density are the sources of crater formation on the surface of the material when it is irradiated by HCPEB. However, in fact, the size of vacancy defects is several orders of magnitude smaller than the size of craters. At the same time, it seems quite probable that in this case tubular micropores with a diameter much smaller than the diameter of the craters could be formed.

This may be the mechanism of porosity formation in HCPEB – irradiated metals and alloys.

2.2. SHRINKAGE POROSITY

In alloys solidifying in the temperature range, crystals growing from the casting surface deeply go into the liquid metal. They form an intermediate two-phase area consisting of solid and liquid metal. Until the crystals growing from the surface meet, the upper layers of liquid metal or lateral gains compensate for the metal shrinkage. However, after the fusion of the growing crystals, the volumes of liquid alloy between them are isolated from each other and the additional feed of liquid metal is stopped. When a liquid alloy solidifies under such conditions, small shrink holes form in the isolated space. The accumulation of small shrink holes is called shrinkage porosity.

As is known that after pulsed electron surface treatment, a remelting area with a thickness ranging from a few micrometers to 100 or more micrometers is formed where, due to the high rate of cooling from the liquid state, ultradisperse and nanoscale structures are formed in most cases [18]. Crystals grow in the direction opposite to the heat sink direction and reach the sample surface from the boundary between the liquid metal and the solid substrate. The crystals typically have dendritic structure inside and consist of packages of equally oriented dendritic grains. Packages of dendrites belonging to different crystals are rotated relative to each other by some angle. Due to the ultra-high rate of melt cooling, dendrites do not have time to develop to the required size and fill the entire space of the layer. Therefore, the gaps between the dendrites remain free, and a system of shrinkage pores is formed. The observation of such shrinkage porosity in the layer remelted by HCPEB irradiation has been reported in several studies [19–21].

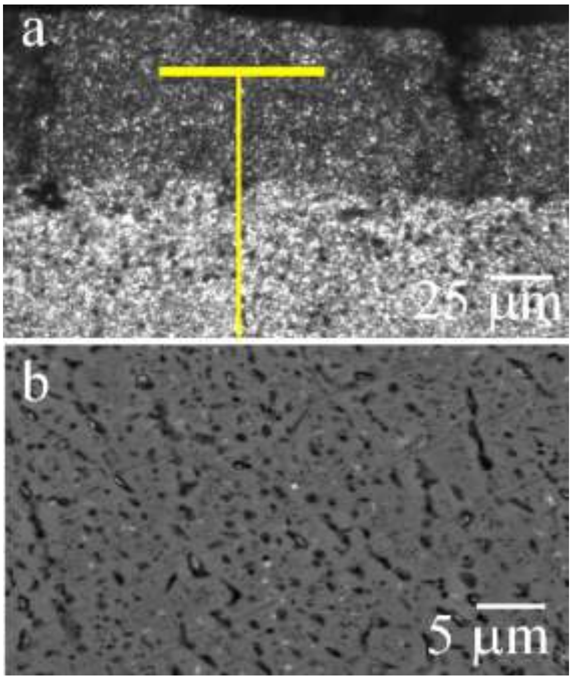

Fig. 2. Cross-sectional view of 1933 alloy in the electron beam treatment area (a); microstructure of the remelted layer at a depth of 30 µm from the surface (b)

Fig. 2,a shows a view of the microstructure of the cross-section in the area of alloy treatment by the electron beam. As can be seen from this figure, the thickness of the remelted surface layer is approximately 100 µm. The analysis of the microstructure view allowed to establish that irradiation of 1933 alloy by pulsed electron beam causes noticeable changes in the structure of its near-surface layer. The structure of the modified layer is nonequilibrium judging from the blurred contrast of grain boundaries. As can be seen from Fig. 2,b, the remelted layer is characterized by the presence of a rather large amount of porosity, whereas porosity was absent in the initial state of the alloy. The appearance of these cavities suggests that they are shrinkage cavities formed as a result of the solidification process. Since their morphology and sizes vary widely, these cavities cannot be confused with diffusion porosity. As noted, for example, in the study [21] greater shrinkage porosity density is characteristic of finer grain size.

2.3. DEFORMATION POROSITY

As is known, as a result of HCPEB action, the dynamic stress field causes the development of intensive deformation processes on the surface of the irradiated material [2, 22, 23]. As it was shown for the first time in studies [24, 25] the intensive stress field arising in the surface layer of AA2024 and 1933 aluminum alloys after exposure to HCPEB is compensated by plastic deformation including by the mechanism of grain-boundary sliding. This is confirmed by the presence on the irradiated surface of wedge-shaped pores and a developed deformation relief characteristic of alloys deformed under conditions where grain boundary sliding is the underlying deformation mechanism.

Fig. 3 shows the surface views of the remelted layer of 1933 and AA2024 alloys after HCPEB treatment. This surface morphology is due to rapid heating, melting and subsequent crystallization and rapid cooling. First of all, these figures show a fine and equiaxial granular structure with a grain size of noticeably 5…7 µm. The formation of such microstructure is induced by HCPEB treatment since in the initial state the alloys have a coarser and unequal grain microstructure. The fact of presence of wedge-shaped pores on this surface (some of them are indicated by arrows) draws attention. Note that a similar morphology of surface porosity can also be observed in study [26], where specimens of the aluminum alloy Al-12.6Si were treated by HCPEB. As it is known [27], the passage of grain boundary sliding processes is the cause of porosity formation observed in Fig. 3. Wedge-type cracks result from sliding inhibition along boundaries at the junction of three grains. It is the porosity of such morphology that is observed in superplastically deformed materials when the main deformation mechanism is grain-boundary sliding [28–31]. The formation of such porosity under superplasticity conditions is a consequence of insufficient accommodation of the grain boundary sliding process.

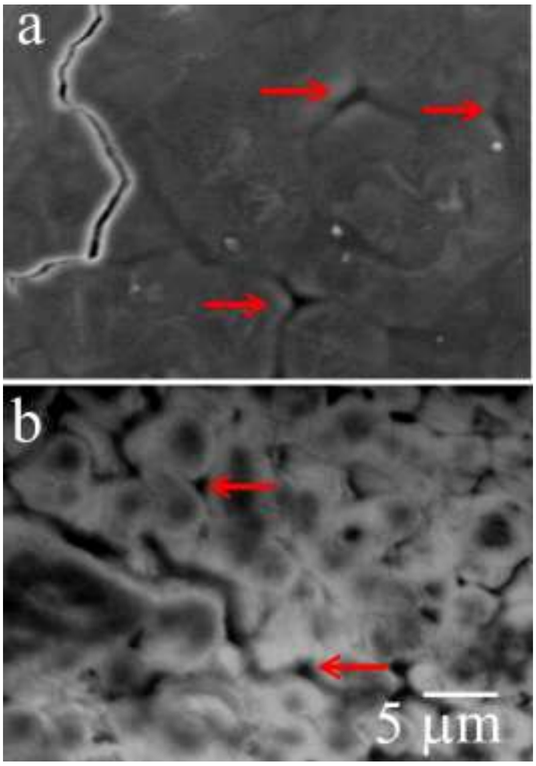

Fig. 3. Surface view of the layer of AA2024 alloy (a) and 1933 alloy (b) remelted by HCPEB irradiation

Grain boundary sliding is a high-temperature process. For its implementation, it is essential that grain boundaries are in an activated state. The presence of local inclusions of liquid phase at grain boundaries may be one of such activated states [31–33]. In the case of 1933 and AA2024 alloys researched in this study, such a state can be implemented during cooling of the HCPEB-molten surface layer, when the inner part of grains will be already crystallized due to liquation processes, while the periphery of grains will still be in the liquid state.

Alloys, unlike pure metals, crystallize not at one temperature, but in the temperature range. At the same time, the composition of crystals formed at the beginning of solidification may differ significantly from the composition of the last portions of the crystallizing solution.The process of grain boundary sliding itself is probably implemented at the moment when the entire molten interlayer has already crystallized, except for insignificant areas at grain boundaries. The resulting thermoelastic stresses will lead to sliding along not yet fully crystallized grain boundaries. Apparently, the thickness of the remelted layer (about 100 μm) plays an important role in the possibility of intergranular deformation implementation in this case. Such thickness allows the development of a grain boundary sliding process in the volume of the remelted layer.

CONCLUSIONS

Three following types of porosity formed in HCPEB-modified layers of various metals and alloys can be distinguished as a result of the conducted studies, as well as based on the analysis of literature data:

1. Vacancy porosity – well-dispersed, tubular, surface-rounded pores with diameters ranging from hundreds of nanometers to a few micrometers, formed by the migration of presaturation vacancies to the surface along grain boundaries and/or through various dislocation configurations.

2. Shrinkage porosity – small, relatively evenly distributed irregularly shaped cavities formed as a result of metal shrinkage during crystallization.

3. Deformation porosity – wedge-shaped, non-uniformly distributed pores formed as a result of the passage of strain induced by dynamic stress fields due to the mechanism of grain boundary sliding.

ACKNOWLEDGEMENTS

The research presented in this article was financially supported by the Simons Foundation International Program: PD-Ukraine: President Directed – Ukraine Support Grants, Record ID: SFI-PD-Ukraine-00014584.

REFERENCES

1. A.D. Pogrebnjak, V.S. Ladysev, N.A. Pogrebnjak, A.D. Michaliov, V.T. Shablya, A.N. Valyaev, A.A. Valyaev, V.B. Loboda. Comparison of radiation damage and mechanical and tribological properties of α-Fe exposed to intense pulsed electron and ion beams // *Vacuum.* 2000, v. 58, N 1, p. 45-52.

2. Y. Qin, J.X. Zou, C. Dong, X.G. Wang, A.M. Wu, Y. Liu, S. Hao, Q. Guan. Temperature-stress fields and related phenomena induced by a high current pulsed electron beam // *Nucl. Instr. Meth. Phys. Res. B.* 2004, v. 225, issue 4, p. 544-542.

3. V.V. Bryukhovetsky, V.F. Klepikov, V.V. Lytvynenko, D.E. Myla, O.A. Startsev, Yu.F. Lonin, A.G. Ponomarev. Formation mechanism of craters on the surface of AA6111 aluminum alloy irradiated by quasi-relativistic high-current electron beam // *Vacuum.* 2023, v. 215, p. 112263.

4. S. Yang, Z. Guo, M. Zhang, Q. Guan, Y. Jin, Y. Liu. Effect of high current pulsed electron beam surface irradiation on the microstructure and electrochemical behavior of zircaloy-4 // *Nucl. Instr. Meth. Phys. Res. B.* 2018, v. 434, p. 81-87.

5. V.V. Bryukhovetsky, V.V. Lytvynenko, D.E. Myla, V.A. Bychko, Yu.F. Lonin, A.G. Ponomarev, V.T. Uvarov. Effect of Structural and Phase Changes under Relativistic Electron Pulsed Beam Irradiation on the Aluminum Alloys Micro-hardness // *Physics and Chemistry of Solid State*. 2021, v. 22, N 4, p. 655-663.

6. Y. Qin, C. Dong, X. Wang, S. Hao, A. Wu, J. Zou, Y. Liu. Temperature profile and crater formation induced in high-current pulsed electron beam processing // *Journal of Vacuum Science and Technology A.* 2003, v. 21, N 6, p. 1934-1938.

7. V.V. Bryukhovetsky, V.V. Lytvynenko, D.E. Myla, Yu.F. Lonin, A.G. Ponomarev, V.T. Uvarov. Strengthening Mechanisms in Surface Layer of Duralumin modified by a High Current Pulsed Relativistic Electron Beam // *J. Nano- and Electronic Physics*. 2021. v. 13, N 6, p. 06025-1 – 06025-6.

8. L. Hu, B. Gao, G. Zhu, Y. Hao, S. Sun, G. Tu. The effect of neodymium on the microcracks generated on the Al-17.5Si alloy surface treated by high current pulsed electron beam // *Applied Surface Science*. 2016, v. 364, p. 490-497.

9. C. Zhang, Y. Zhang, N. Tian, S. Chen, Z. Qian, P. Lv, Q. Guan. Microstructures of pure nickel induced by high-current pulsed electron beam irradiation // *Protection of Metals and Physical Chemistry of Surfaces.* 2016, v. 52, p. 869-875.

10. Z. Zhang, S. Yang, P. Lv, Y. Li, X. Wang, X. Hou, Q. Guan, The microstructures and corrosion properties of polycrystalline copper induced by high-current pulsed electron beam // *Applied surface science.* 2014, v. 294, p. 9-14.

11. Y. Zou, J. Cai, M.Z. Wan, P. Lv, Q.F. Guan. Formation mechanism of micropores on the surface of pure aluminum induced by high-current pulsed electron beam irradiation // *Chinese Physics Letters.* 2011, v. 28, N 11, p. 116102.

12. D.E. Myla, V.V. Bryukhovetsky, V.V. Lytvynenko, V.P. Poyda, A.V. Poyda, V.F. Klepikov, V.T. Uvarov, Yu.F. Lonin, A.G. Ponomarev. Analysis of changes in the phase and structural state of the surface layer of an aluminum alloy 1933, melted by a pulsed electron beam // *Problems of Atomic Science and Technology.* 2020, N 2(126), p. 33-38.

13. V.V. Bryukhovetsky, V.F. Klepikov, V.V. Lytvynenko, D.E. Myla, Yu.F. Lonin, A.G. Ponomarev. The Structural Phase State and Strength Properties of the Surface Layer of AA6111-T4 Aluminum Alloy Irradiated by the High-Current Electron Beam // *Nucl. Instr. Meth. Phys. Res. B.* 2022, v. 519, p. 1-8.

14. D.E. Myla, V.V. Bryukhovetsky, V.V. Lytvynenko, S.I. Petrushenko, O.O. Nevgasimov, Yu.F. Lonin, A.G. Ponomarev V.T. Uvarov. Microstructure and property modifications in surface layers of a AA6111 aluminum alloy induced by high-current pulsed relativistic electron beam // *Problems of Atomic Science and Technology*. 2022, N 2(138), p. 25-31.

15. Q. Guan, X. Wang, J. Zhu, K. Chen, L. Liang, Q. Zhang, C. Dong. Fabrication of Micropore on AISI 304L Austenitic Stainless Steel Surface by High-current Pulsed Electron Beams Irradiation // *ISIJ International*. 2009, v. 49, p. 1449-1451.

16. S. Yang, J. Cai, P. Lv, C. Zhang, W. Huang, Q. Guan. Microstructures and properties of zirconium-702 irradiated by high current pulsed electron beam // *Nucl. Instr. Meth. Phys. Res. B.* 2015, v. 358, p. 151-159.

17. A.D. Pogrebnjak, A.D. Mikhaliov, N.A. Pogrebnjak, Yu.V. Tsvintarnaya, V.I. Lavrentiev, M. Iljashenko, A.N. Valyaev, S. Bratushka, A. Zecca, R. Sandrik. Evolution of vacancy defects and dislocations in surface layers of iron as a result of pulsed electron beam treatment // *Phys. Lett. A.* 1998, v. 241, p. 357-363.

18. B. Gao, K. Li, P. Xing. Formation of a double-layer ultrafine crystal structure for high-current pulsed electron beam-treated Al-20Si-5Mg alloy // *Coatings.* 2019, v. 9, N 7, p. 413.

19. J. Zou, K. Zhang, T. Grosdidier, C. Dong. Analysis of the evaporation and re-condensation processes induced by pulsed beam treatments // *International Journal of Heat and Mass Transfer.* 2013, v. 64, p. 1172-1182.

20. P. Yan, T. Grosdidier, X. Zhang, J. Zou. Formation of large grains by epitaxial and abnormal growth at the surface of pulsed electron beam treated metallic samples // *Materials and Design*. 2018, v. 159, p. 1-10.

21. K.M. Zhang, J.X. Zou, T. Grosdidier, N. Gey, S. Weber, D.Z. Yang, C. Dong. Mechanisms of structural evolutions associated with the high current pulsed electron beam treatment of a NiTi shape memory alloy // *J. Vac. Sci. Technol. A.* 2007, v. 25, N 1, p. 28-36.

22. K.M. Zhang, J.X. Zou, B. Bolle, T. Grosdidier. Evolution of residual stress states in surface layers of an AISI D2 steel treated by low energy high current pulsed electron beam // *Vacuun*. 2013, v. 87, p. 60-68.

23. J. Cai, L. Ji, S.Z. Yang, X.T. Wang, Y. Li, X.L. Hou, Q.F. Guan. Deformation mechanism and microstructures on polycrystalline aluminum induced by high-current pulsed electron beam // *Chinese Science Bulletin.* 2013, v. 58, p. 2507-2511.

24. V.V. Bryukhovetsky, V.V. Lytvynenko, D.E. Myla, V.V. Shatov, A.G. Ponomarev, O.L. Rak, V.A. Bychko. Residua stresses and deformation mechanisms in the surface layer of AA1933 aluminum alloy induced by high-current pulsed electron beam // *Problems of Atomic Science and Technology*. 2024, N 2(150), p. 34-40.

25. V.V. Bryukhovetsky, V.V. Lytvynenko, O.A. Startsev, D.E. Myla, Yu.N. Volkov, O.L. Rak. Mechanisms of deformation induced by high-current pulsed electron beam irradiation // *Materials Letters*. 2024, v. 367, p. 136642.

26. Y. Hao, B. Gao, G.F. Tu, H. Cao, S.Z. Hao, C. Dong. Surface modification of Al–12.6 Si alloy by high current pulsed electron beam // *Applied Surface Science.* 2012, v. 258, N 6, p. 2052-2056.

27. J. Intrater, E.S. Machlin. Grain boundary sliding and intercrystalline cracking // *Acta metallurgica.* 1959, v. 7, N 2, p. 140-143.

28. V.V. Bryukhovetskii, V.P. Poida, A.V. Poida, R.I. Kuznetsova, K.A. Mahmoud, D.E. Pedun. Phase transformations and structural changes in the course of the high_temperature superplastic deformation of aluminum alloys // *Phys. Met. Metallogr*. 2010. v. 110, N 6, p. 588-596.

29 V.V. Bryukhovetskij. On the origin of high-temperature superplasticity of a coarse-grained avial-type aluminum alloy // *Fizika Metallov i Metallovedenie*. 2001, v. 92, issue 1, p. 107-111 (in Russian).

30. V.V. Bryukhovetskyy, V.P. Pojda, A.V. Poyda, D.R. Avramets', R.I. Kuznetsova, O.P. Kryshtal', O.L. Samsonnik, K.A. Mahmud. Mechanical properties and structural changes during superplastic deformation of 6111 aluminium alloy // *Metallofiz. Noveishie Tekhnol.* 2009, v. 31, issue 9, p. 1289-1302 (in Russian).

31. A.V. Pojda, V.V. Bryukhovets'ky, D.L. Voronov, R.I. Kuznetsova, V.F. Klepikov. Superplastic behaviour of an AlMg6 alloy at the high homological temperatures // *Metallofiz. Noveishie Tekhnol.* 2005, v. 27, issue 3, p. 317-330 (in Russian).

32. V.P. Pojda, V.V. Bryukhovets'ky, R.I. Kuznetsova, A.V. Pojda, V.F. Klepikov. Formation and development of the fibre structures during superplastic deformation of matrix aluminium alloys // *Metallofiz.*

Noveishie Tekhnol. 2003, v. 25, issue 1, p. 117-132 (in Russian).

33. V.V. Bryukhovetsky, D.E. Myla, V.P. Poyda, A.V. Poyda. Effect of Homogenization on the Superplasticity and Microsuperplasticity of the Al-Zn-Mg-Cu Aluminum Alloy // *J. Nano- and Electronic Physics*. 2020, v. 12, N 6, p. 06025-1 – 06025-8.

Article received 21.08.2025

ОСОБЛИВОСТІ УТВОРЕННЯ МІКРОПОРИСТОСТІ ПРИ ОПРОМІНЕННІ АЛЮМІНІЄВИХ СПЛАВІВ СИЛЬНОСТРУМОВИМИ ІМПУЛЬСНИМИ ПУЧКАМИ ЕЛЕКТРОНІВ

В.В. Брюховецький, Д.Є. Мила, В.В. Шатов, О.Л. Рак, В.А. Бичко

Охарактеризовано різні типи поверхневої мікропористості, що виникає при опроміненні металів і сплавів сильнострумовими імпульсними пучками електронів. Виділено три типи такої пористості: вакансійна, усадочна та деформаційна. Наведено характерні види такої мікропористості. Проаналізовано механізми утворення кожного з перерахованих типів мікропористості. Обговорюється значення цих спостережень для більш глибокого розуміння структурно-фазових перетворень, що відбуваються при опроміненні металів та сплавів імпульсними пучками електронів.